J|A|C|S
COMMUNICATIONS

Published on Web 05/05/2007

Bi_2Te_3/Te Multiple Heterostructure Nanowire Arrays Formed by Confined Precipitation

Wei Wang, Xiaoli Lu, Tao Zhang, Genqiang Zhang, Wenjun Jiang, and Xiaoguang Li*

Hefei National Laboratory for Physical Sciences at Microscale, Department of Physics, University of Science and Technology of China, Hefei 230026, P. R. China

Received February 11, 2007; E-mail: lixg@ustc.edu.cn

The fabrication of advanced thermoelectric materials with high figures of merit (ZT) holds a considerable technological promise for device applications.[1] In bulk compounds, such as $AgPb_mSbTe_{2+m}$ thermoelectric materials exhibit an impressive high ZT of ~2.2 at 800 K,[2] related to the reduced lattice thermal conductivity (κ_L) by the embedded nanostructured precipitates.[3] On the other hand, the low-dimensional systems offer remarkable advantage for ZT enhancement[4] owing to the sharper density of states and increased phonon scattering. Until now, the highest ZT of ~2.4 was reported by Venkatasubramanian et al. in Bi_2Te_3/Sb_2Te_3 superlattice film.[5] Since a larger enhancement in ZT is anticipated with decreasing the dimensionality, the heterostructure nanowires (zero-dimensional) are predicted to exhibit a better thermoelectric performance than conventional nanowires or superlattice films,[6] attracting more and more attention. Many efforts have been made for preparing the heterostructure nanowires by means of the vapor−liquid−solid (VLS)[7] or the pulsed electrodeposition processes.[8] For example, Yang et al. developed a Hybrid pulsed laser ablation/chemical vapor deposition (PLA−CVD) method for synthesizing the high-quality Si/SiGe nanowires with a reduced κ_L.[7b,9] However, it is still a challenge to find a simple and universal strategy with a high degree of control for fabricating the thermoelectric heterostructure nanowires.

The bismuth−tellurium alloy system has been a focus of extensive research because of its excellent thermoelectric performance near room temperature.[10] Here, we report a novel and convenient route for the spontaneous formation of the Bi_2Te_3/Te multiple heterostructure nanowire arrays using the precipitation reaction of the supersaturated $Bi_{0.26}Te_{0.74}$ alloy under a nanoconfined system. The porous anodic alumina (PAA) membranes, fabricated via a standard two-step anodization process,[11] act as the nanoscale reaction tubes to provide the physically confined environment. The Bi−Te alloy was deposited into PAA membranes at a constant current of 1.5 mA by a potentiostat/galvanostat (HDV-7C) with the electrolyte solution containing 5×10^{-2} M $HTeO_2^+$ and 1.25×10^{-2} M Bi^{3+} (the detailed synthetic procedure is presented in the Supporting Information Part 1). Then the as-deposited nanowire arrays were annealed under vacuum at a set temperature to obtain the final products. The morphologies of the as-prepared sample were investigated by high-resolution transmission electron microscopy (HRTEM, JEOL 2010) and field-emission scanning electron microscopy (FE-SEM, JEOL JSM-6700F). The structures and compositions were confirmed by HRTEM, selected-area electron diffraction (SAED), and energy dispersive X-ray spectroscopy (EDS).

Figures 1a and b show the FE-SEM and TEM images of the sample annealed at 300 °C for 300 min. Large scale nanowire arrays with lengths up to tens of micrometers can be observed, and the TEM image of the dispersed nanowires shows that those nanowires

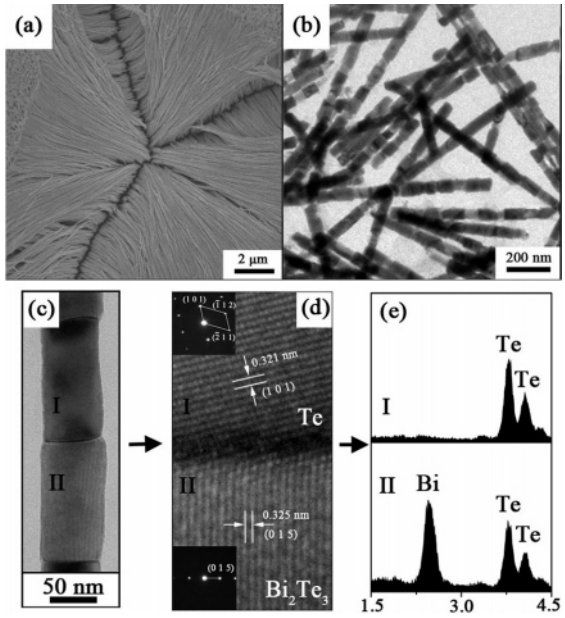

Figure 1. (a) FE-SEM image of the Bi_2Te_3/Te nanowire arrays, (b) TEM image of the dispersed Bi_2Te_3/Te heterostructure nanowires, (c) the close-up of a couple of segments, (d) HRTEM image and SAED patterns of each segment, (e) the EDS results of each segment.

with high-aspect ratios are straight and continuous. The diameter of the nanowire is about 60 nm, which corresponds closely to the size of the nanochannel of the PAA membranes. It is noted that each nanowire exhibits periodic heterogeneous contrast obviously. The length of each segment ranges from 50 to 100 nm, and the interface between neighboring segments is well perpendicular to the wire axis.

From the close-up of a couple of segments in a randomly selected nanowire in Figure 1c, the interface clearly shows a junction structure. The corresponding SAED patterns and HRTEM results shown in Figure 1d indicate the single crystalline nature of each segment. The upper pattern of segment I can be steadily indexed to (101), ($\bar{1}$12), ($\bar{2}$11) as a hexagonal Te phase (JCPDS 04-0554), and the lower pattern of segment II can be assigned to (015) as a hexagonal Bi_2Te_3 phase (JCPDS 82-0358) (The structure of the segment II can be well characterized by rotating a certain angle with the sample hold, see the Supporting Information Part 2). Moreover, the EDS results of each segment, shown in Figure 1e, also provide a powerful evidence that the segment I is pure Te, and the segment II is the alloy with the atomic ratio of about 41% Bi versus 59% Te, which is exactly close to the stoichiometric Bi_2Te_3 as the equilibrium phase in the Bi−Te phase diagram.[12] These results strongly support the nature of the

10.1021/ja070976c CCC: $37.00

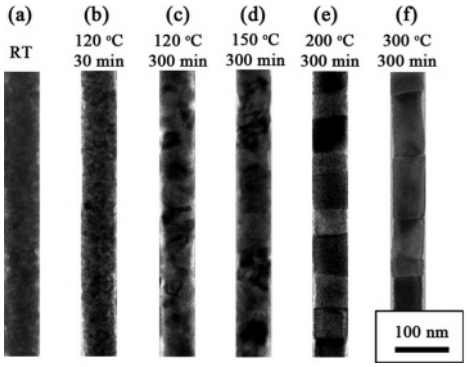

Figure 2. TEM images of the samples annealed under different conditions.

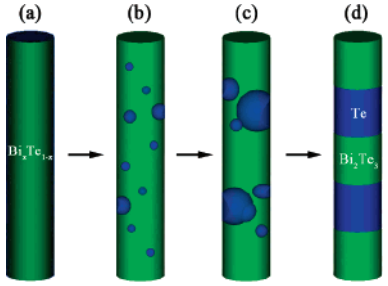

Figure 3. Schematic diagram of the formation process of Bi_2Te_3/Te heterostructure nanowires.

precipitation reaction of the supersaturated Bi−Te alloy, which can be formulated as

$$Bi_xTe_{1-x}(x < 0.4) \xrightarrow{\Delta} \frac{x}{2}Bi_2Te_3 + \left(1 - \frac{5x}{2}\right)Te \qquad (1)$$

To understand the formation mechanism of these heterostructure nanowires, on the basis of the differential scanning calorimetry (DSC, Perkin-Elmer Diamond DSC) and X-ray diffraction (XRD, Philip X'pert) analyses (see the Supporting Information Part 3), the transformation process was carefully studied by the microstructure evolution of the nanowires annealed at 120, 150, 200, and 300 °C. As shown in Figure 2a, the as-deposited samples almost exhibit no diffraction contrast along the nanowire. While at the early annealing stage at 120 °C for 30 min, the appearance of the dense heterogeneous contrast, demonstrated in Figure 2b, indicates the onset of the precipitation. As the reaction time prolongs to 300 min, the heterogeneous contrast becomes clear with irregular black regions in sizes of about 30−40 nm, as shown in Figure 2c. With increasing annealing temperature, the black regions grow larger, and the periodic blocks with heterogeneous contrast start to form in the sample annealed at 200 °C, which trend to be larger at higher temperature (see Figure 2d,e,f). However, this multiple heterostructure nanowires will be decomposed when the temperature reaches 400 °C (see the Supporting Information Part 4).

On the basis of the above analyses, the formation process can be regarded as following the classical precipitation in alloy system, consisting of three stages: nucleation, growth, and coarsening process, as shown schematically in Figure 3. With increasing temperature, a large number of Te crystal nuclei would be precipitated from the homogeneous supersaturated Bi−Te alloy nanowires at the beginning of the thermal treatment, and the crystal nuclei will grow by absorbing Te continuously with further reaction, as illustrated in Figure 3a,b,c. It is well-known that, after a precipitate reaction has ended, the microstructure would be coarsened by sacrificing the smaller Te grains for decreasing the total interfacial area and hence the free energy.[13] According to the Lifshitz−Slyozov−Wagner (LSW) theory,[14] in the same annealing time the average grain size will increase with increasing temperature. But, when the grains grow as large as the nanochannel size, their growth will be limited in the two-dimensional (2-D) vertical plane of the nanowire because of the confinement of the nanochannels in PAA membranes. It is considered that the grains can grow into a block, arranged equally in the nanowires, which builds the block-by-block structure within a nanochannel, as shown in Figure 3d. To minimize the free energy with the smallest interfacial area, it should obviously give a flat interface between blocks instead of a curved one. As a result, the well-established Bi_2Te_3/Te heterostructure nanowire arrays are fabricated.

In summary, we successfully synthesized the Bi_2Te_3/Te multiple heterostructure nanowire arrays through a simple annealing process of the supersaturated Bi−Te nanowire arrays. The heterostructure nanowires, as the block-by-block structure, may be derived from the precipitation confined by the nanochannels of the PAA membrane. This work provides a facile and cheap strategy for synthesizing multiple heterostructure nanowire arrays.

Acknowledgment. This work was supported by the National Natural Science Foundation of China (Grant 50421201) and the National Basic Research Program of China (Grant 2006CB922005).

Supporting Information Available: The detailed synthetic procedures, microstructure analysis, thermal characterization results, and the decomposition process analysis. This material is available free of charge via the Internet at http://pubs.acs.org.

References

(1) (a) DiSalvo, F. J. *Science* **1999**, *285*, 703−706. (b) Tritt, T. M. *Science* **1999**, *283*, 804−805.
(2) Hsu, K. F.; Loo, S.; Guo, F.; Chen, W.; Dyck, J. S.; Uher, C.; Hogan, T.; Polychroniadis, E. K.; Kanatzidis, M. G. *Science* **2004**, *303*, 818−821.
(3) (a) Quarez, E.; Hsu, K. F.; Pcionek, R.; Frangis, N.; Polychroniadis, E. K.; Kanatzidis, M. G. *J. Am. Chem. Soc.* **2005**, *127*, 9177−9190. (b) Poudeu, P. F. P.; D'Angelo, J.; Kong, H. J.; Downey, A.; Short, J. L.; Pcionek, R.; Hogan, T. P.; Uher, C.; Kanatzidis, M. G. *J. Am. Chem. Soc.* **2006**, *128*, 14347−14355.
(4) Hicks, L. D.; Dresslhaus, M. S. *Phys. Rev. B* **1993**, *15*, 12727−12731.
(5) Venkatasubramanian, R.; Siivola, E.; Colpitts, T.; O'Quinn, B. *Nature* **2001**, *413*, 597−602.
(6) (a) Lin, Y. M.; Dresselhaus, M. S. *Phys. Rev. B* **2003**, *68*, 075304. (b) Dames, C.; Chen, G. *J. Appl. Phys.* **2004**, *95*, 682−693.
(7) (a) Björk, M. T.; Ohlsson, B. J.; Sass, T.; Persson, A. I.; Thelander, C.; Magnusson, M. H.; Deppert, K.; Wallenberg, L. R.; Samuelson, L. *Nano Lett.* **2002**, *2*, 87−89. (b) Wu, Y. Y.; Fan, R.; Yang, P. D.; *Nano Lett.* **2002**, *2*, 83−86. (c) Gudiksen, M. S.; Lauhon, L. J.; Wang, J. F.; Smith, D. C.; Lieber, C. M. *Nature* **2002**, *415*, 617−620.
(8) (a) Piraux, L.; George, J. M.; Despres, J. F.; Leroy, C.; Ferain, E.; Legras, R.; Ounadjela, K.; Fert, A. *Appl. Phys. Lett.* **1994**, *65*, 2484−2486. (b) Xue, F. H.; Fei, G. T.; Wu, B.; Cui, P.; Zhang, L. D. *J. Am. Chem. Soc.* **2005**, *127*, 15348−15349. (c) Yoo, B. Y.; Xiao, F.; Bozhilov, K. N.; Herman, J.; Ryan, M. A.; Myung, N. V. *Adv. Mater.* **2007**, *19*, 296−299.
(9) Li, D. Y.; Wu, Y. Y.; Fan, R.; Yang, P. D.; Majumdar, A. *Appl. Phys. Lett.* **2003**, *83*, 3186−3188.
(10) (a) Prieto, A. L.; Sander, M. S.; Martín-González, M. S.; Gronsky, R.; Snads, T.; Stacy, A. M. *J. Am. Chem. Soc.* **2001**, *123*, 7160−7161. (b) Jin, C. G.; Xiang, X. Q.; Jia, C.; Liu, W. F.; Cai, W. L.; Yao, L. Z.; Li, X. G. *J. Phys. Chem. B* **2004**, *108*, 1844−1847. (c) Zhou, J. H.; Jin, C. G.; Seol, J. H.; Li, X. G.; Shi, L. *Appl. Phys. Lett.* **2005**, *87*, 133109.
(11) Masuda, H.; Fukuda, K. *Science* **1995**, *268*, 1466−1468.
(12) Yu, J. Q.; Yi, W. Z.; Chen, B. D.; Chen, H. J. *A Collection of the Binary alloy States*; Shanghai Science and Technology Press: Shanghai, China, 1987.
(13) Christian, J. W. *The Theory of Transformations in Metals and Alloys;* Pergamon Press: Oxford, 2002.
(14) (a) Lifshitz, I. M.; Slyozov, V. V. *J. Phys. Chem. Solids* **1961**, *19*, 35−50. (b) Wanger, C. *Z. Elektrochem.* **1961**, *65*, 581−594.

JA070976C